

# Fractal Analysis of Dental Radiographic Images in the Irregular Regions of Interest

Edward Oczeretko, Marta Borowska, Izabela Szarmach, Agnieszka Kitlas, Janusz Szarmach, and Andrzej Radwański

**Abstract.** The irregularity or "roughness" of medical images is quantified by means of fractal dimension  $D$ . For medical images diagnostically important information often lies in the texture. In this paper we describe the application of the intensity difference scaling method for assessment of the fractal dimension  $D$  in the irregular regions of interest (irregular ROI-s). Near boundary between different tissues or structures the values of fractal dimensions changed significantly. It is difficult to fit entire regular region of interest within the examined organ with simultaneous inclusion of the relevant fragment, and at the same time to avoid the influence of boundaries.

## 1 Introduction

Fractals, a concept of the last decades have been successfully applied in many areas of science and technology. One of the most prominent applications is fractal analysis in medicine, especially in modelling of tissues and organs constitution, analysis of different kinds of images and time sequences [13, 16]. Medical images can be treated as surfaces with the intensity at each pixel. For radiological, magnetic

---

Edward Oczeretko · Marta Borowska · Agnieszka Kitlas · Andrzej Radwański

Department of Medical Informatics, University of Białystok, Sosnowa 64,

15-887 Białystok Poland

e-mail: eddoczer@ii.uwb.edu.pl, mborowska@ii.uwb.edu.pl,

akitlas@ii.uwb.edu.pl, ara2n@wp.pl

Izabela Szarmach

Department of Orthodontics, Medical University of Białystok, Waszyngtona 15A,

15-274 Białystok Poland

e-mail: izaszarmacgr@gmail.com

Janusz Szarmach

Department of Maxillofacial Surgery, Medical University of Białystok,

M. Skłodowskiej-Curie 24A, 15-274 Białystok Poland

e-mail: zchs@umwb.edu.pl

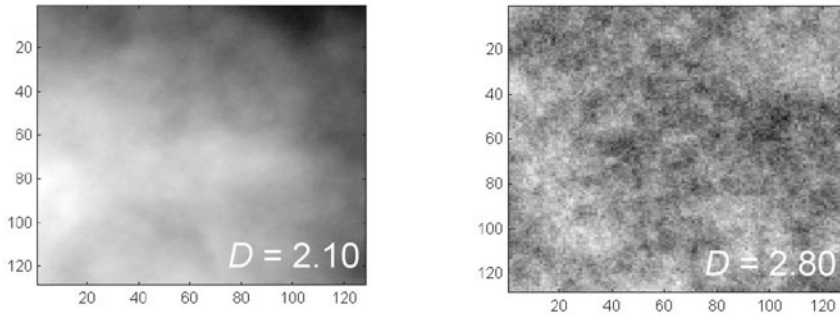


**Fig. 1** Synthetic fractal textures with fractal dimension  $D = 2.10$  and  $2.80$ . These surfaces were generated by means of Matlab function `synth2`, that is a part of `FracLab`, a Fractal Analysis Software ([www.scilab.org](http://www.scilab.org)).

resonance or ultrasonic images the grey levels estimate the intensity. For different surfaces the values of the fractal dimension are in the range between 2 and 3. The smooth surface is characterized by fractal dimension of about 2; the rougher surfaces have higher fractal dimensions. The fractal dimension may be used as an index of heterogeneity (Fig. 1). Generally, fractals are the sets for which the Hausdorff–Besicovitch dimension, or the fractal dimension  $D$  are greater than topological dimension. The fractal dimension may be calculated in many ways since Hausdorff–Besicovitch’s definition is too complicated for practical estimation [9, 2]. Hausdorff definition is a mathematical foundation of various methods of the fractal dimension estimating. Thus, according to various algorithms, there are various kinds of fractal dimension. Thus we can use various algorithms to assess the fractal dimension of medical images. For all the methods, the relationship between selected parameters is governed by a power-law:

$$M(\varepsilon) = C \cdot \varepsilon^{\text{exponent}}, \quad (1)$$

where  $M(\varepsilon)$  is a result of measurements,  $\varepsilon$  is a scale,  $C$  — is a constant, *exponent* — there is a direct relationship between the exponent and the value of the fractal dimension. Among the algorithms for the calculation of fractal dimension of surfaces are:

- rectangular prism surface area method [4];
- triangular prism surface area method [7];
- power spectral density method [8];
- methods based on mathematical morphology: flat structuring element method [10], and cover blanket method [11];
- dispersion analysis [1];
- variogram analysis [3];
- intensity difference scaling method [5];
- box dimension [6].

These methods were applied in the analysis of various kinds of medical images [12, 13, 14]. In all the cases the studies were performed in regular regions of interest (regular ROI-s) — mostly square regions. Calculation of fractal dimension in irregular regions of interest was described two times in the literature [17, 18]. We showed that in the case of the lung scintigrams,  $D = 2.23$  in the region containing the boundary of the organ and  $D = 2.59$  within the organ. In order to avoid the influence of the boundaries, and other structures it would be proper to calculate the fractal dimensions in irregular ROI-s. The aim of this study was to show the validity of assessment of fractal dimension in irregular regions of interest, where  $D$  can be calculated by means of the intensity difference scaling method.

## 2 Practical Assessment of Fractal Dimension

In this chapter three methods of calculations of fractal dimension are presented: rectangular prism surface area method ("skyscraper method"), triangular prism surface area method, and intensity difference scaling method.

### 2.1 Rectangular Prism Surface Area Method — "Skyscraper Method"

Medical images can be treated as surfaces with the intensity  $I(x, y)$  at each point  $(x, y)$ . For nuclear medicine images, the intensity is a number of counts of gamma radiation quantum, whereas for radiological or ultrasonic images the gray levels estimate the intensity. Fig. 2a shows this idea of the "skyscraper" model of medical image [4]. For each element of image matrix  $(x, y)$  there is a rectangular prism  $\varepsilon \cdot \varepsilon \cdot I(x, y)$ , where  $\varepsilon$  is the length of pixels creating a single element of image matrix. Assuming  $\varepsilon = 1$  is more convenient for our calculation. The area  $S(\varepsilon)$  of such "skyscraper" surface is expressed by the sum of the areas of the roofs plus the sum of the exposed walls of the rectangular prisms:

$$S(\varepsilon) = \sum_{x,y} \varepsilon^2 + \sum_{x,y} \varepsilon [|I(x, y) - I(x + 1, y)| + |I(x, y) - I(x, y + 1)|] \quad (2)$$

$S(\varepsilon)$  was calculated for  $\varepsilon = 1$ . Afterwards the numbers of counts were averaged for adjacent four elements of the image matrix ( $\varepsilon = 2$ ) to form a new image matrix and  $S(\varepsilon)$  was computed. Repeating this averaging process we calculated  $S(\varepsilon)$  for  $\varepsilon = 4, 8, 16$  and so on. The matrix of the investigated image must be square. The empirical relationship between  $S(\varepsilon)$  and  $\varepsilon$  is:

$$S(\varepsilon) = C \cdot \varepsilon^{2-D}, \quad (3)$$

where  $C$  is a constant,  $D$  is the fractal dimension. Values of  $D$  can be obtained using least-squares linear regression to estimate the slope of line of  $S(\varepsilon)$  versus  $\varepsilon$  in ln-ln scale.

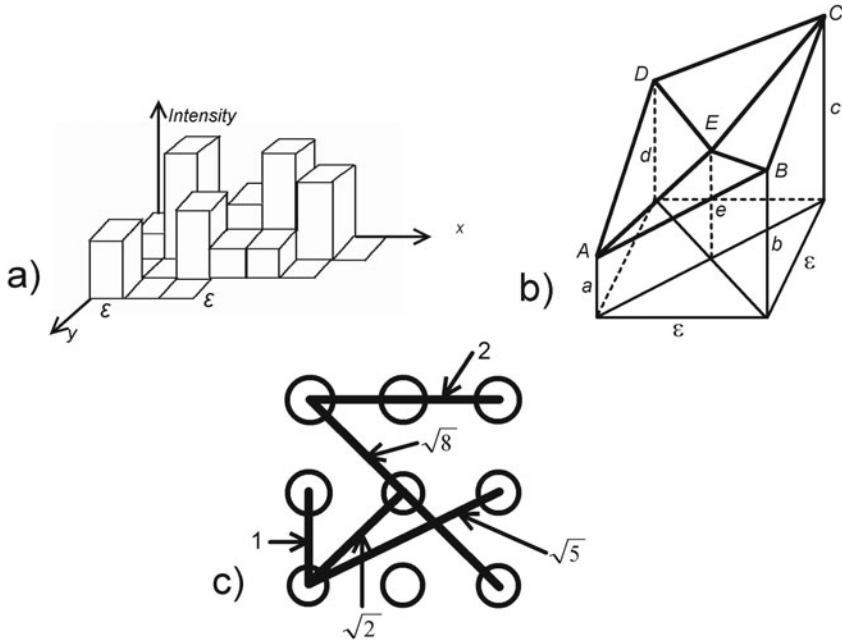


**Fig. 2** a) The "skyscraper" model of medical image, b) Creation of triangular prism, c)  $3 \times 3$  image. There are 5 possible scales. The total number of pixel pairs for these scales is 38.

### 2.2 Triangular Prism Surface Area Method

The idea of triangular prism surface area method is presented on Fig. 2b. Let  $a, b, c$  and  $d$  represent the number of counts in four adjacent pixels,  $e$  is the mean,  $e = (a + b + c + d)/4$ . The area of surface  $S(\epsilon)$  is the sum of areas of triangles  $DCE$ ,  $DAE$ ,  $ABE$  and  $CBE$  [7]. We calculate the  $S(\epsilon)$  for all image. By repeating this for different size of squares, the relationship (3) between the total area and the spacing of squares is used to estimate the fractal dimension. Here the image matrix must have the shape of a square.

### 2.3 Intensity Difference Scaling Method

For given  $M \times M$  image the multi-scale intensity difference vector  $IDV$  is defined as follows [5]:

$$MIDV = [id(1), id(2), id(3), \dots, id(smax)], \tag{4}$$

where  $smax$  is the maximum possible scale,  $id(s)$  is the average of the absolute intensity difference of all pixel pairs with scale  $s$ .

$$cd(s) = \frac{1}{N_s} \sum_{x_1=0}^{M-1} \sum_{y_1=0}^{M-1} \sum_{x_2=0}^{M-1} \sum_{y_2=0}^{M-1} |I(x_2, y_2) - I(x_1, y_1)|, \tag{5}$$

where  $I(x_1, y_1)$  and  $I(x_2, y_2)$  are two pixels in the image with intensity values between 0 and 255;  $N_s$  is the number of pixel pairs for scale  $s$ , scale  $s$  (distance between two pixels):

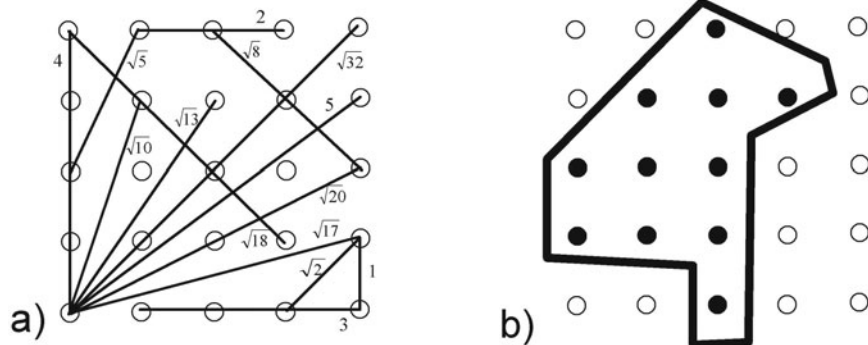
$$s = \sqrt{(x_2 - x_1)^2 + (y_2 - y_1)^2} \tag{6}$$

Fig. 2c shows  $3 \times 3$  image. There are 5 possible scales, 5 possible distances between pixels. The total number of pixel pairs analyzed for these scales is 36. For  $27 \times 27$  images the number of all scales is 314, for  $63 \times 63$  images the number of all scales is 1529, and the total number of pixel pairs analyzed for these scales is 31505922. To reduce the number of elements of *MIDV* vector, normalized *NMIDV* vector was used in which only integer scales occurred. Non-integer scales were not lost. For example, information from scales:  $\sqrt{5}$ ,  $\sqrt{8}$ , (2.2361, 2.8284) was included in scale 2. For fractal surfaces the relationship between *MIDV* and scale  $s$  is governed by a power-law:

$$MIDV = C \cdot s^{3-D} \tag{7}$$

### 3 Irregular Regions of Interest

By means of the intensity difference scaling method we could assess the values of fractal dimension in irregular ROI-s, which is impossible by means of other algorithms. Fig. 3a shows the  $5 \times 5$  image with 25 pixels and 14 possible scales. The total number of pixel pairs analyzed for these scales is 300. Fig. 3b illustrates manually drawn irregular region of interest **R** with 11 pixels and 9 possible scales. In calculation only pixels belonging to regions **R** were used.



**Fig. 3** a)  $5 \times 5$  image. There are 14 possible scales. The total number of pixel pairs analyzed for these scales is 300. b) Manually drawn irregular region of interest with 11 pixels and 9 possible scales.

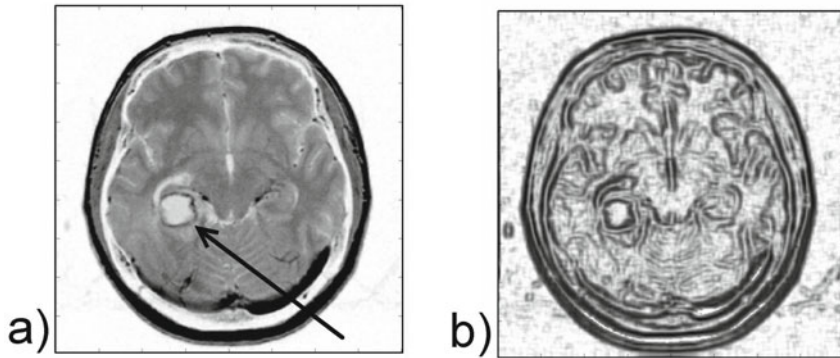


**Fig. 4** a) Original MR images (the arrow shows the tumor), b) Transformed images in which the value of each pixel is the fractal dimension

## 4 Experiments – Intensity Difference Scaling Method

Program for fractal analysis was written in Visual Basic (Microsoft .NET Framework 3.5).

### 4.1 *Magnetic Resonance Image*

Magnetic resonance (MR) image of the brain was obtained using 1.5T MR scanner (Picker Edge Eclipse) with standard circulatory polarized head coil. We calculated fractal dimension over the whole  $512 \times 512$  image in each pixel by calculating the dimension of a  $9 \times 9$  pixel block centered on that pixel. In the obtained images the value of each pixel was the fractal dimension. Fig. 4a illustrates an original  $512 \times 512$  image (the arrow shows the tumour). Fig. 4b shows transformed image in which the value of each pixel is the fractal dimension. The tumour is more obvious. The edges of other structures were enhancement too.

By means of the fractal analysis we can detect and enhance edges in the analyzed image, which may a diagnostic significance. Near boundary between different tissues or structures the values of fractal dimensions changed significantly, which enables edge enhancement.

### 4.2 *Pantomogram (Panoramic Radiograph)*

Pantomogram is a panoramic radiographic record obtained by a pantomograph. It shows maxillary and mandibular dental arches and their associate structures. Pantomograms were digitized with an Umax Alpha Vista II scanner (LaserSoft Imaging Inc., USA), interfaced through a scan software program (SilverFast Applications) to a computer. Fig. 5a shows the pantomogram with two marked regular regions. Figures 5b and 5c show the regular regions of interest from Fig. 5a. Inside of these

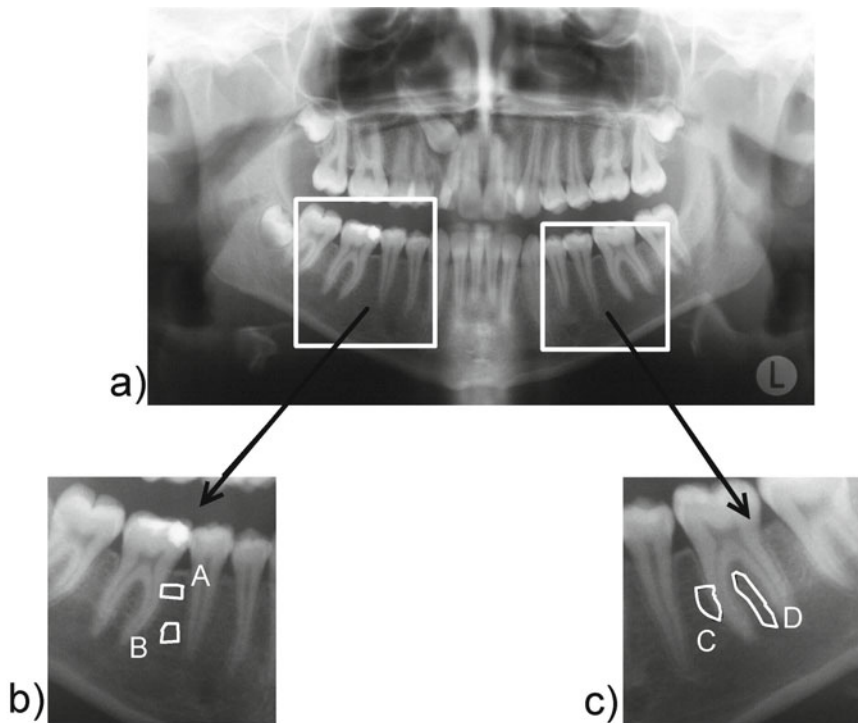


**Fig. 5** a) Panoramic radiograph with marked two regular regions, b, c) Regular regions with marked irregular ROI-s

**Table 1** Results of fractal analysis in irregular regions of interest (Fig. 5b and Fig. 5c)

Irregular Regions	Fractal dimension $D$	Number of scales	Number of pixel pairs
A	2.461	1891	2377290
B	2.848	4005	8110378
C	2.313	3160	4286846
D	2.777	6903	7689081

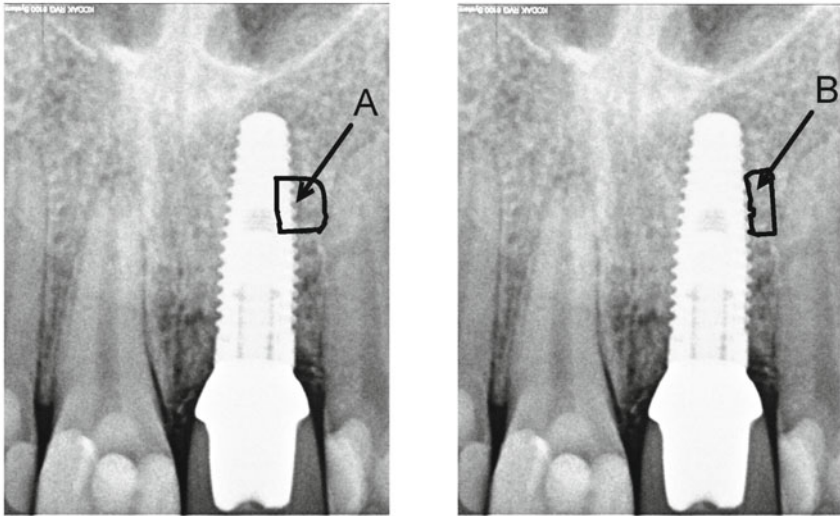
regions irregular ROI-s A, B, C and D were marked. Table 1 shows the results of fractal analysis in the irregular regions. When the irregular ROI contain the boundaries and fragment of the teeth the value of fractal dimension is relatively low.

### 4.3 Dental Radiovisiographic Image

The study was based on the analysis of radiovisiogram of patient treated with prosthetic implants in a private dental practice due to a missing tooth. In the patient,

**Table 2** Results of fractal analysis in irregular regions of interest (Fig. 6)

Irregular Regions	Fractal dimension $D$	Number of scales	Number of pixel pairs
A	2.306	7626	265054121
B	2.596	10878	31541653

**Fig. 6** Radiovisiographic images with marked two irregular regions A and B. Irregular region B was drawn close to the implant, but it did not contain the elements of the implant.

Nobel Biocare implant was used — intraosseous, screw-type, made up of pure titanium (99.75% titanium, 0.05% iron, 0.1% oxygen, 0.03% nitrogen, 0.05% carbon, 0.012% hydrogen). X-ray picture was obtained using a KODAK RVG 6100 set. Radiovisiogram was done after 6 months after implantation. Table 2 summarizes the results of fractal analysis of irregular region of interest (Fig. 6). When the irregular ROI contain the boundary and fragment of the implant the value of fractal dimension is low ( $D = 2.306$ ).

## 5 Conclusions

Medical images are often complex, irregular and noisy. The diagnostic information often lies in the texture. In the case of dental radiographic images the boundaries of the analyzed structures change significantly the values of fractal dimension. It is difficult to fit the entire regular region of interest within the examined organ with simultaneous inclusion of the relevant fragment avoiding the influence of boundaries



and other kinds of unnecessary structures at the same time. Our method of assessment of fractal dimension in irregular regions of interest solves these difficulties.

## References

1. Bassingthwaighte, J.B.: Physiological heterogeneity, fractals link determinism and randomness in structures and functions. *News Physiol. Sci.* 3, 5–10 (1988)
2. Besicovitch, A.: On the fundamental properties of linearly measurable plane sets of points. *Math. Ann.* 98, 422–464 (1928)
3. Bianchi, F., Bonetto, R.: FERimage: an interactive program for fractal dimension,  $d(\text{per})$  and  $d(\text{min})$  calculations. *Scanning* 23, 193–197 (2001)
4. Caldwell, C.B., Moran, E.L., Bogoch, E.R.: Fractal dimension as a measure of altered trabecular bone in experimental inflammatory arthritis. *J. Bone Miner Res.* 13(6), 978–985 (1998)
5. Chen, C.C., Daponte, J.S., Fox, M.D.: Fractal feature analysis and classification in medical imaging. *IEEE Trans. Med. Imaging* 8, 133–142 (1989)
6. Chen, S.S., Keller, J.M., Crownover, R.M.: On the calculations of fractal features from images. *IEEE Trans. Patt. Anal. Machine Intell.* 15(10), 1087–1090 (1993)
7. Clarke, K.C.: Computation of the fractal dimension of topographic surfaces using the triangular prism surface area method. *Comp. Geosci.* 12, 713–722 (1986)
8. Dennis, T.J., Dessipris, N.G.: Fractal modelling in image texture analysis. *IEEE Proc.-F* 136, 227–235 (1989)
9. Hausdorff, F.: Dimension und äußeres Maß. *Math. Ann.* 79, 157–179 (1918)
10. Maragos, P., Sun, F.-K.: Measuring the fractal dimension of signals: morphological covers and iterative optimization. *IEEE Trans. Signal Process.* 41(1), 108–121 (1993)
11. Peleg, S., Naor, J., Hartley, R., Avnir, D.: Multiple resolution texture analysis and classification. *IEEE Trans. Pattern Anal. Mach. Intell.* 6(4), 518–523 (1984)
12. Losa, G.A., Merlini, D., Nonnemacher, T.F., Weibel, E.R.: *Fractals in Biology and Medicine*, vol. II. Birkhäuser Verlag, Basel (1998)
13. Losa, G.A., Merlini, D., Nonnemacher, T.F., Weibel, E.R.: *Fractals in Biology and Medicine*, vol. III. Birkhäuser Verlag, Basel (2002)
14. Losa, G.A., Merlini, D., Nonnemacher, T.F., Weibel, E.R.: *Fractals in Biology and Medicine*, vol. IV. Birkhäuser Verlag, Basel (2005)
15. Umbaugh, S.E.: *Computer vision and image processing: A practical approach using CVIP tools*. Prentice Hall PTR, Upper Saddle River (1998)
16. Oczeretko, E.: Wymiar fraktalny w analizie sygnałów i obrazów biomedycznych. Wydawnictwo Uniwersytetu w Białymstoku, Białystok (2006) (in Polish)
17. Oczeretko, E., Rogowski, F., Jurgilewicz, D.: Fractal analysis of nuclear medicine scans. In: Losa, G.A., Merlini, D., Nonnemacher, T.F., Weibel, E.R. (eds.) *Fractals in Biology and Medicine*, vol. II. Birkhäuser, Basel (1998)
18. Oczeretko, E., Borowska, M., Kitlas, A., Borusiewicz, A., Sobolewska-Siemieniuk, M.: Fractal analysis of medical images in the irregular regions of interest. In: 8th IEEE International Conference on Bioinformatics and BioEngineering, Athens, CD, October 8–10 (2008), ISBN: 978-1-4244-2845-8